DEVELOPMENT OF A MOLECULAR DYNAMICS MODEL OF THERMAL REACTIVITY IN POLYMERS

by

Marc R. Nyden
Building and Fire Research Laboratory
National Institute of Standards and Technology
Gaithersburg, MD 20899, USA

Reprinted from the 9th Annual BCC Conference on Flame Retardancy, June 1-3, 1998, Stamford, CT, 1-22 pp. Proceedings. 1998.

Development of a Molecular Dynamics Model of Thermal Reactivity in Polymers*†

Marc R. Nyden
Building and Fire Research Laboratory
National Institute of Standards and Technology
Gaithersburg, MD 20899
mnyden@nist.gov

Introduction

Thermal reactivity is an important consideration that impacts the way polymers and the materials that are made from them are processed and used. This realization has provided motivation for the development of a predictive model that can simulate the chemical behavior of large molecules at high temperatures. The research conducted in this laboratory has focused on the application of molecular modeling techniques to identify factors that affect the condensed phase thermal degradation chemistry of polymers in ways that result in a reduction in their flammability [1,2,3,4,5]. This effort has culminated in the development of a novel computer program, hereafter called MD_REACT, based on molecular dynamics (MD). The feature that distinguishes MD_REACT from other MD codes is that it allows for the formation of new bonds from free radical fragments that are generated when bonds in the polymer break and, thereby, accounts for the chemical reactions that play a major role in the thermal degradation process.

The purpose of this paper is to provide an overview of the progress we have made in the development of an integrated model that possesses the capability to model thermal degradation in a wide range of polymers. The strategy employed to accomplish this objective was to make use of an inter-process communications protocol (IPC) to pass coordinates, forces and connectivity information between MD_REACT, which computes the reactive

force field, and Discover 95, a commercially available molecular dynamics code offered by Molecular Simulations (MSI) [6], which updates the molecular structure on the basis of the solution to the equations of motion.

What follows is an overview of the theory and implementation of MD_REACT. This exposition is highlighted with results from recent applications performed as part of a general survey of fire retarded polymers. Included in this survey are blends of polypropylene with silica gel, three representative bromine-containing additives, and a polypropylene/graphite layered nanocomposite. Some preliminary results from a model validation study of the rate of beta-scission reactions in a small gas phase molecule (n-pentane) are also presented.

Theory

Molecular Dynamics

The basis of MD_REACT is molecular dynamics. This technique consists of solving Hamilton's equations of motion

$$\frac{\partial H}{\partial p_i} = \frac{dq_i}{dt}, \qquad \frac{\partial H}{\partial q_i} = -\frac{dp_i}{dt}, \tag{1}$$

for each of the 3N molecular degrees of freedom. In this equation p_i and q_i denote the Cartesian components of momentum and position, respectively. The Hamiltonian of the model polymers considered in the present investigation is based on the Centralized Valence Forcefield (CVFF) distributed with Discover 95 [7].

$$\begin{aligned} H = \sum_{i}^{3N} \frac{p_i^2}{2m_i} + \sum_{ij}^{nbonds} V_b(r_{ij}) \\ + \sum_{ijk}^{nangles} V_a(\theta_{ijk}) \\ + \sum_{ijkl}^{ntorsions} V_t(\phi_{ijkl}) + \sum_{ij}^{npairs} V_{nb}(r_{ij}) \end{aligned} \tag{2}$$

The first term on the right hand side of Eq. (**2**) represents the kinetic energy of the N atoms

in the model polymer. The next terms are the potential energies for bond stretching (V_b), bending (V_a), and a torsional potential (V_t) that restricts internal rotation around the covalent bonds. The last term represents the nonbond potential energy (V_{nb}) resulting from the interactions between all pairs of atoms that are not part of the same covalent bond angle (*i.e.* between atoms that are separated by at least two atoms).

The energy required to stretch the covalent bonds is represented by the Morse potential in Eq.(3).

$$V_b = S(ij)\{D[1 - \exp(-\alpha(r - r_e))]^2 - D\} \qquad (3)$$

In this equation, r is the distance between bonded atoms i and j, r_e is the equilibrium bond length, D is the amount of energy required to dissociate the bond, and $\alpha = [k_b/(2D)]^{1/2}$. The force constant, k_b, is defined as

$$k_b = \left(\frac{\partial^2 V_b}{\partial r^2}\right)_{r=r_e}. \qquad (4)$$

The role of the switching functions, S(ij), is discussed below.

The potential energy for bond bending is represented by

$$V_a = S(ij)S(jk)k_\theta(\theta - \theta_e)^2. \qquad (5)$$

Where θ denotes the angle determined from the dot product of the normalized bond vectors between three adjacent atoms (i, j and k). The force constant, k_θ, is defined, in analogous fashion to k_b, as the second derivative of the potential energy evaluated at the equilibrium bond angle (Θ_e).

Rotations about covalent bonds are restricted by the torsional potential

$$V_t = S(ij)S(jk)S(kl)k_\phi[1 + \cos(n\phi - \phi_e)]. \qquad (6)$$

The dihedral angle, ϕ, is defined by the three bond vectors between four adjacent atoms (i,j,k and l). The parameters, k_Φ, n, and ϕ_e determine the height, multiplicity, and position of the

barrier to internal rotation.

The nonbond potential energy consists of two terms corresponding to the Van der Waals and electrostatic interactions. These are represented by

$$V_{nb} = \varepsilon[(\frac{r^*}{r})^{12} - 2(\frac{r^*}{r})^6] + \frac{\delta_i \delta_j}{r}. \qquad (7)$$

Where δ_i and δ_j are the partial charges on nonbonded atoms separated by a distance, r. The parameters r^* and ε in the Van der Waals term determine the position of the minimum and the depth of the potential well, respectively.

Unimolecular Reactions

The reactions that are responsible for most of the mass loss during the thermal degradation of polymers are hydrogen transfer and beta-scission. Obviously, the credibility of our model for predicting the thermal stability and flammability of polymers would be questionable if it failed to provide reasonable estimates for the rate constants of these reactions. In this paper, we test the predictive capability of the model by comparing the computed rate constant for beta-scission in n-pentyl radical to the experimental value at 1250 K. A more complete investigation that addresses the kinetic competition between beta-scission and hydrogen transfer in small gas phase molecules is in progress.

Hydrogen transfer and beta-scission reactions, which also occur in small gas phase molecules that can be studied in detail, are known to proceed via the unimolecular mechanism summarized in Eq.(8).

$$\begin{array}{c} \overset{k_e}{A + M \underset{k_{de}}{\longleftrightarrow} A^* + M} \\ A^* \xrightarrow{k_{uni}} P \end{array} \qquad (8)$$

The asterisk is used to indicate that the molecule is thermally excited by collisions with other molecules (M). Once excited, the molecule can either be deactivated by another collision, or undergo unimolecular decomposition to products (P). When the frequency of collision is high, the rate of deactivation would be expected to be much greater than the rate of unimolecular decomposition. In mathematical terms, we have $k_{de}[M][A^*] >> k_{uni}[A^*]$, which defines the high pressure limit. The corresponding rate expression is given by

$$R_\infty(E,T) = K_{eq}(E,T)k_{uni}(E)[A] \quad (9)$$

Where

$$K_{eq}(E,T) = \frac{[A^*]}{[A]}.$$

In Eq.(9), E is the total energy of the molecule and the brackets are used to denote concentration. In the case of small gas phase molecules at low temperatures, [A] >> [A^*] and

$$K_{eq}(E,T) \approx \frac{[A]^*}{[A]+[A]^*} = P(E,T). \quad (10)$$

The distribution function

$$P(E,T) = \frac{E^{S-1}\exp(-\frac{E}{k_BT})}{\Gamma(S)(k_BT)^S} \quad (11)$$

is the classical probability that a molecule in equilibrium with a reservoir at temperature, T, has an energy, E [8]. In this equation, S = 3N - 6 is the number of vibrational degrees of freedom in the molecule, k_B is the Boltzmann constant, T is the absolute temperature, and $\Gamma(S)$ is the gamma function which is equal to (S-1)!.

The high pressure rate constant is obtained by integration of the energy dependent rate expression in Eq.(9) over all E > E_0. This gives

$$k_\infty(T) = \int_{E0}^{\infty} P(E,T)k_{uni}(E)dE = \omega\exp(-\frac{E_0}{k_BT}). \quad (12)$$

Where ω is a constant that corresponds to the frequency of energy exchange between the vibrational modes and E_0 is the minimum or critical energy required for the unimolecular reaction. Thus, the experimental high pressure rate constant corresponds to the microcanonical ensemble average of the unimolecular rate constant.

A more detailed understanding of the nature of this integral may be gained by substitution of the analytical expression for the unimolecular rate constant

$$k_{uni}(E) = \omega(1 - \frac{E_0}{E})^{S-1} \qquad (13)$$

derived from RRK theory [8] into Eq.(12). The reason for invoking the RRK formula, rather than the more accurate RRKM theory [9], is that it provides an analytical expression for the number of states that is more appropriate for comparison with classical molecular dynamics. It should be noted, however, that we only make use of the RRK formula to provide information about the shape of the integrand in Eq.(12). The actual evaluations of $k_{uni}(E)$, used in the determination of the rate constants reported below, are obtained directly from the MD simulations as

$$k_{uni}(E) = \frac{\Delta n_r}{\Delta t_r}. \qquad (14)$$

Where, E is the excitation energy and Δn_r is the number of reactions that occur in the time interval, Δt_r.

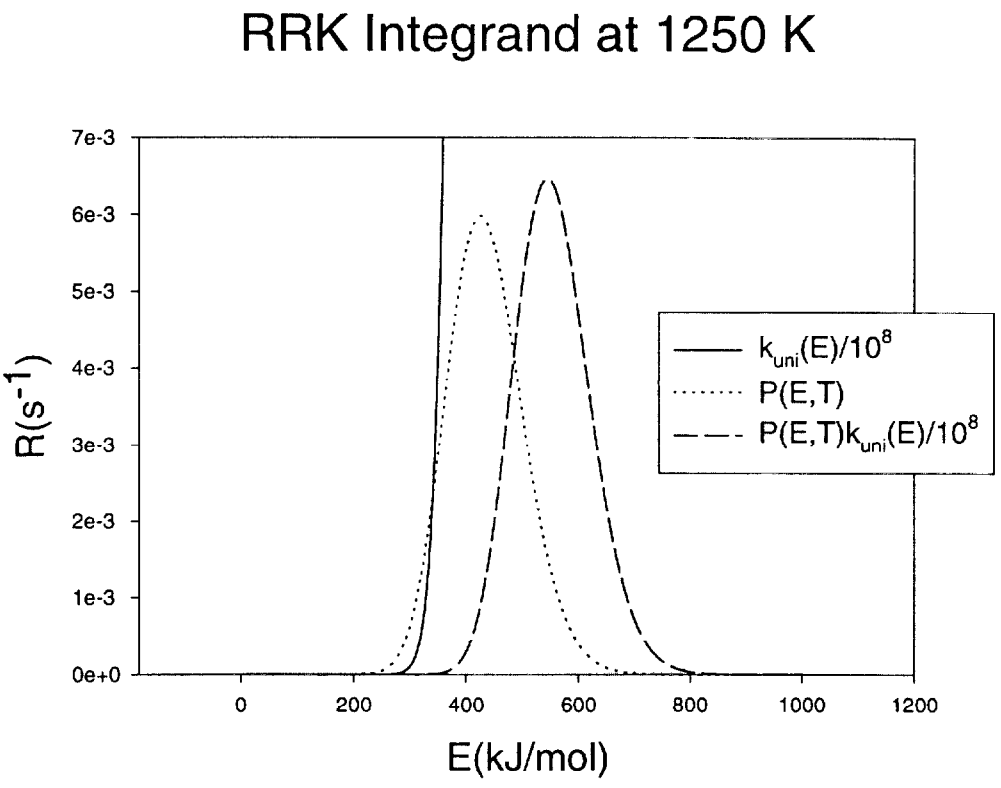

Figure 1. The integrand corresponds to the small region of overlap between $k_{uni}(E)$ and P(E,T).

The integrand in Eq.(12) is a sharply peaked function with a pronounced maximum at

$$E_{max} = (S-1)k_B T + E_0 \qquad (15)$$

that results from the small region of overlap between $k_{uni}(E)$ and the tail of P(E,T) (figure 1). The offset from the average thermal energy, $E_{avg} = (S\text{-}1)k_B T$, is a consequence of the fact that molecules having energies less than E_0 cannot react.

The sharp fall-off that characterizes the RRK integrand implies that it should be possible to approximate $k_\infty(T)$ from data obtained from a small number of simulations corresponding to a narrow range of energies in the vicinity of the maximum. Indeed, the situation is even more favorable in the application to polymers where $S \rightarrow \infty$. In this case, the number of degrees of freedom is large so that $E_{avg} >> E_0$ and all of the polymers have sufficient energy to react. Thus, assuming that $K_{eq}(E,T) = [A^*]/[A] = 1$ and that the fluctuations from the average thermal energy are negligible (again because there are so many vibrational modes), we obtain

$$\lim_{S\to\infty} k_\infty(T) = \int_{E_{avg}-\delta}^{E_{avg}+\delta} K_{eq}(E,T)k_{uni}(E)dE \approx k_{uni}(E_{avg}). \qquad (16)$$

The basis of these assumptions is that, in polymers, the collisions that activate and deactivate the molecule are largely intra-molecular events. From this point of view, it may be argued that the mechanism for beta-scission more closely approaches unimolecularity in polymers than it does in small gas phase molecules, where the activation reactions are actually bimolecular. Furthermore, since $(1- E_0/E_{avg})^{S-1} \approx \exp(-(S-1)E_0/E_{avg})$ when $E_0/E_{avg} \rightarrow 0$, Eq.(16) reduces to

$$\lim_{S\to\infty} k_\infty(T) \approx k_{uni}(E_{avg}) \approx \omega(1-\frac{E_0}{E_{avg}})^{(s-1)} \approx \omega\exp(\frac{-E_0}{k_B T}). \qquad (17)$$

This is the familiar Ahrrenius rate expression which is consistent with the observed temperature dependence of high pressure rate constants for unimolecular reactions in small gas phase molecules. The analysis presented here, however, indicates that, in the case of polymers, $k_\infty(T)$ is equal to $k_{uni}(E)$. This is not an unexpected result. It is a simple consequence of the fact that the polymer behaves like the average of its molecular fragments. In principle, this analysis implies that only a single MD simulation is needed to evaluate the rate constant for beta-scission in a polymer at a specific temperature. The rate constants

corresponding to the temperature range that is appropriate for polymer degradation (600 - 900 K) may be estimated by extrapolation of Eq.(17) using kinetic parameters determined from a small number of MD simulations performed at high temperatures, where the rate constants are large and the simulation times are correspondingly short.

A straightforward generalization of this analysis to account for the possibility that there may be multiple sites for beta-scission on the same molecule, suggests that the rate constant in Eq.(17) should be multiplied by the number of critical bonds. Thus, although the amount of computer time required to compute the trajectory increases with the size of the molecule under consideration, the amount of time between beta-scission reactions decreases, and the application of the model to polymers remains feasible.

Implementation

Reactions

Bond dissociation and formation are simulated in MD_REACT by the following algorithm. A list of the free radical sites, that are generated when bonds in the polymer break, is updated at every time step. These free radicals are eligible to react with each other to form new bonds. The specific criterion used in MD_REACT is that the atoms participating in a covalent bond become free radicals when the bond stretching energy, V_b, comes within k_BT of dissociation. The program generates a new set of bonds consisting of all possible covalent interactions between the available free radicals and retains those corresponding to the lowest energy subject to the constraints imposed by the atomic valence. This is accomplished by invoking a section of code that sorts the potential bonds in order of increasing energy and accepts new bonds until the valence of the participating atoms is filled. This ensures that there are never more than 4 bonds to any carbon atom, more than 1 bond to any hydrogen atom, and so on. Of course, the number of bonds to an atom can, and frequently does, decrease from its maximum value as a result of bond scission reactions. The bond table in Discover 95 is modified and the trajectory of the polymer is updated accordingly.

In this way, the model accounts for many of the reaction pathways that are involved in the thermal degradation of polymers [10]. Some of these reactions are illustrated, using polypropylene as the prototype, in Figure 2. Listed from top to bottom, these are: random scission, which initiates the thermal degradation process, beta-scission and hydrogen transfer, which constitute the propagation reactions, and a variety of termination reactions including cyclization, intermolecular crosslinking and radical recombination.

Reactive Forcefield

The switching functions, S(ij) in Eqs.(3), (5) and (6), are used to turn the stretching, bending and twisting forces on and off as the corresponding bonds are formed and broken. It

Reaction Pathways

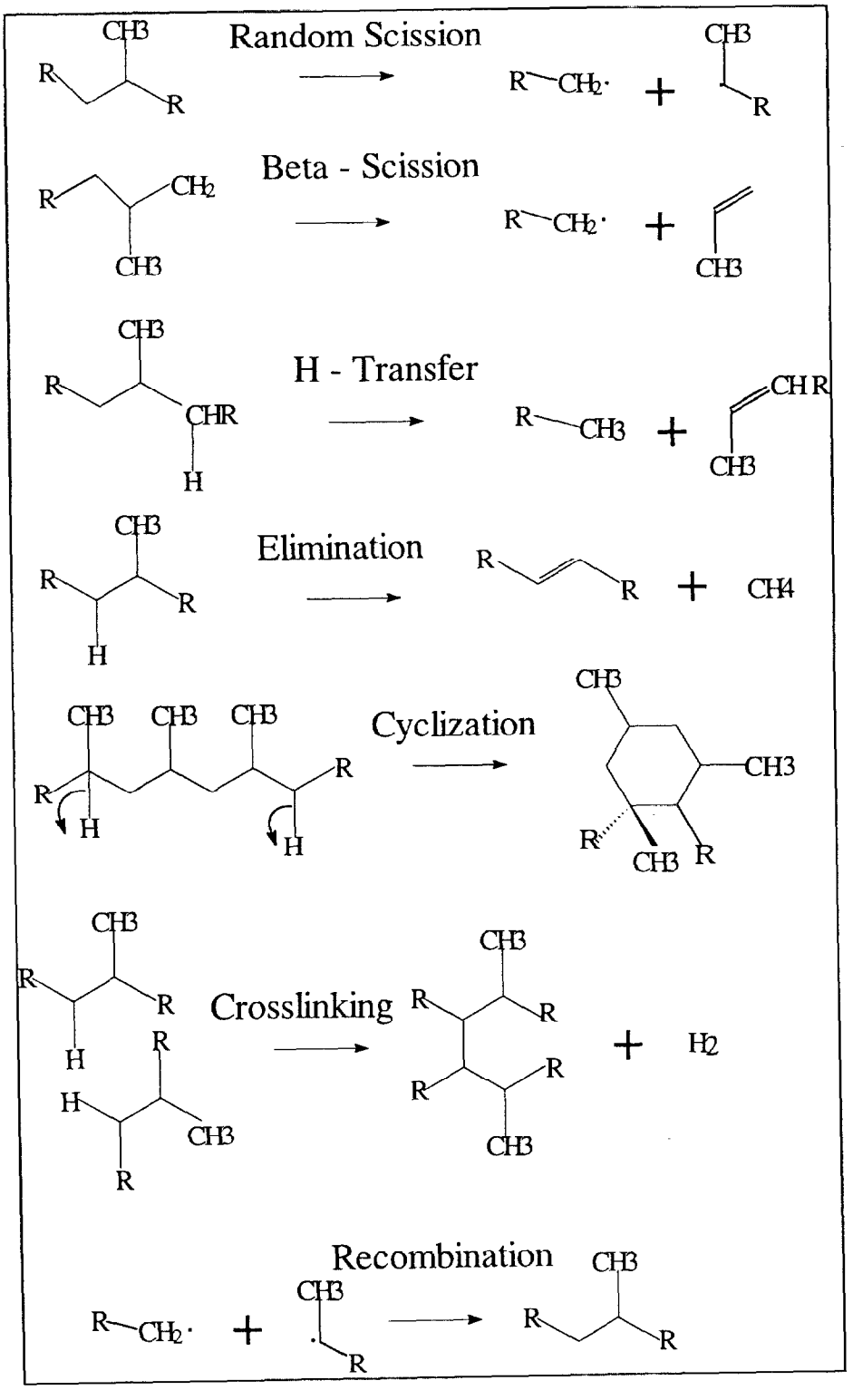

Figure 2. Major reaction pathways in the thermal degradation of polymers.

is the presence of these terms that distinguishes the reactive forcefield used in MD_REACT from the CVFF and other conventional forcefields.

The switching functions used in previous versions of MD_REACT were based on the hyperbolic tangent function in Eq.(18).

$$S(ij) = \frac{1}{2}(1 - \tanh(a(r_{ij} - r_d))) \qquad (18)$$

The justification for using this functional form is that it has the character of a step function, while preserving continuity of the derivatives that are needed for the evaluation of the forces. The parameters a = 40 nm^{-1} and r_d, which is the inter-atomic distance at which the energy in the bond is within kT of dissociation, determine the sharpness and the position of the transition from S = 1 to S = 0, respectively. In the most recent version of MD_REACT, fractional bond orders, as defined in Eq.(19), are used to switch the forces.

$$S(ij) = \begin{cases} 1 & r \le r_e \\ \dfrac{-V_b(ij)}{D(ij)} & r > r_e \end{cases} \qquad (19)$$

This formulation facilitates the description of hypervalent transistion states for hydrogen transfer and similar reactions that play a major role in the thermal degradation process.

Periodic Boundary Conditions

Periodic boundary conditions are implemented by enclosing the model polymer in a unit cell with dimensions that are consistent with the experimental density. The bulk system is simulated by accounting for interactions between the atoms in the polymer and ghost atoms that are created by replicating the unit cell in space (see Figure 8). This makes it possible to maintain realistic densities during simulations of the thermal degradation of isolated chains. The use of periodic boundary conditions also facilitates the assessment of thermal stability, since the rate of mass loss from the degrading polymer can be computed by tabulating the mass of the fragments diffusing outside of the central unit cell as a function of time.

Interface to Discover 95

The interface to Discover 95 is established using the IPC protocol developed by MSI. The input file for the Discover 95 run contains a BTCL [11] command string that initializes an IPC connection in server mode and launches MD_REACT as an external process. A series of database operations that identify and replace the high energy bonds are executed at every

time step. The energy and forces calculated in Discover 95 do not include the contributions due to the presence of the switching functions in Eqs.(3), (5) and (6). These corrections are computed in MD_REACT and passed to Discover 95 in the form of a BTCL restraint.

Computer Experiments

Pentyl Radical

The rate of beta-scission was computed on the basis of the results obtained from MD simulations of the thermal motions of n-pentyl radical over a time period of about 5 x 10^{-9} s. The time spanned by these simulations corresponds to more than 10^4 vibrations of the critical bond; each of which may be viewed as an independent experiment.

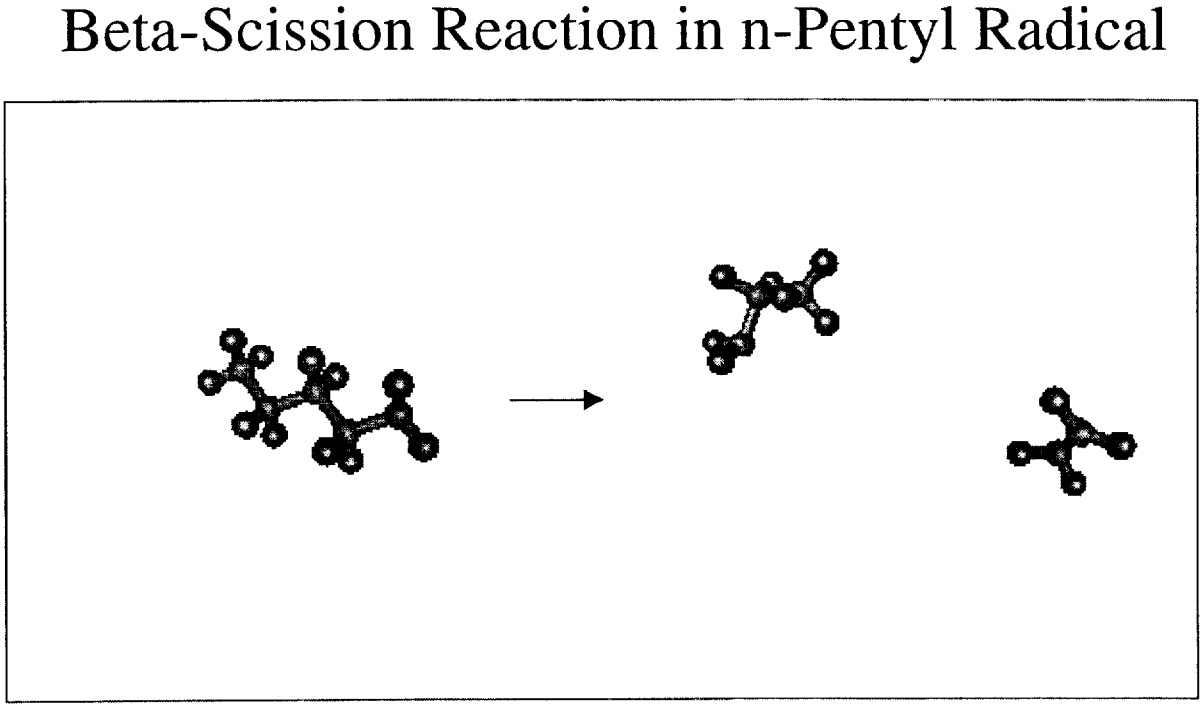

Figure 3. Still frames taken at the beginning (left) and end (right) of a simulation.

The simulations were performed as single molecule MD calculations (*i.e.* without periodic boundary conditions) at a constant energy until the reaction occurred. A mean excitation energy of 544 ± 42 kJ/mol, which corresponds to the maximum of the RRK integrand at 1250 K (Eq.(13)), was obtained by initiating the simulations from a Boltzmann velocity distribution at 1600 K. The conformations of the pentyl radical at the onset of the simulations and just after a beta-scission occurred are compared in Figure 3.

The rate constant for beta-scission was obtained from a three-point integration of

Eq.(12). The end points for the numerical integration were chosen to provide the best triangular fit to the RRK integrand at 1250 K. The result is given in Eq.(20).

$$k(1250K) = (\Delta E)k_{uni}(544)P(544,1250) = (2.2 \pm 0.02)\, x10^{8} s^{-1}. \qquad (20)$$

Where, k_{uni}(544 kJ/mol) = 8.2 x 10^8 s^{-1} was obtained by substitution of the mean reaction time from the simulations into Eq.(14), P(544 kJ/mol, 1250 K) = 1.6 x 10^{-3} mol/kJ, and ΔE = 170 kJ/mol, is the width of the RRK distribution. The uncertainty was estimated by propagating the standard deviation of the energy in Eq.(12).

The computed rate constant in Eq.(20) should be compared to the experimental value of 1.1 x 10^8 s^{-1}. This result was obtained by extrapolating the rate expression derived from shock tube measurements made over the temperature range from 850 - 1000 K [12] to 1250 K. While the order of magnitude agreement suggests that we are on the right track, the factor of two discrepancy implies that there are additional sources of error. Included in the list of possibilities is the inaccuracy resulting from the use of classical dynamics to simulate chemical reactions that, in reality, are quantum events. This may be an important consideration in the hydrogen transfer reactions where the contribution due to tunneling may be significant. In the case of the beta-scission reaction, however, it is more likely that discrepancy is due to errors in the numerical integration that could result if the maximum of the energy dependent rate constant does not coincide with the RRK prediction in Eq.(13). This hypothesis will be examined in the future by performing additional calculations to reveal the true nature of the integrand in Eq.(12).

Silica Gel

Results obtained from experimental studies conducted in this laboratory have indicated that the flammability of polypropylene and other polymers is reduced by the addition of small quantities of silica gel (~ 10% of the total mass) [13]. The effect of silica gel on the thermal degradation of polypropylene was investigated by comparing the results of simulations in the presence and absence of this additive.

The model polymer consisted of 4 chains of isotactic polypropylene each containing 48 propylene monomers (Figure 4). Two models of the silica gel, one with 81 SiO_4 moieties and a maximum pore diameter of 10 Å and the other with 215 SiO_4 moieties and a maximum pore diameter of 30 Å, were examined in an effort to determine the effect of pore diameter on the thermal degradation of the polymer. The initial geometries for the polymer/silica systems were obtained by minimizing the CVFF energies until the maximum derivative was

Model Polymer

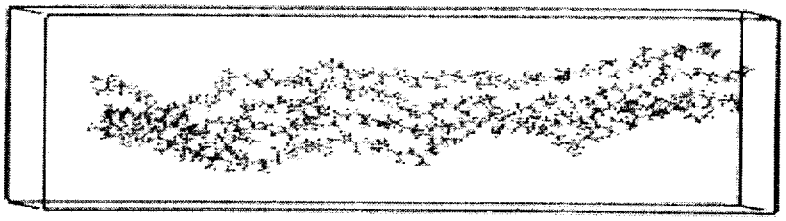

Figure 4. The model polymer consisting of 4 chains each comprised of 48 propylene monomers.

less than 4.2 J/(mol Å) using the Polak Ribiere conjugate gradient algorithm in Discover 95 [11].

The simulations were performed with periodic boundary conditions in two steps. First, a population of free radical polymer fragments was generated by integrating the equations of motion over a constant temperature path at 1500 K for 50 x 10^{-15} s (50 time steps) using the full CVFF forcefield with cross terms coupling adjacent bonds, angles and torsions. The purpose of including cross terms was to facilitate an efficient transfer of thermal energy into the stretching modes that are responsible for bond dissociation. The reactive dynamics were then carried out at a constant temperature of 873 K for 5.0 x 10^{-12} s (5000 time steps) using the reactive forcefield described above. Only the atoms in the polypropylene were dynamic. The positions and connectivities of the Si, O and H atoms in the silica were fixed throughout the simulations. This was done to make the simulations more computationally tractable. Benchmark studies, where these atoms were free to move, indicated that the deformations from the initial structures were minor and that the strategy of constraining the movement of the silica was, therefore, a realistic approximation.

Cone calorimeter measurements on polypropylene/silica gel blends have indicated that pore diameter has a significant effect on the rate-of-heat released from the burning polymer

[13]. In fact, the range of pore diameters spanned by our models is about an order of magnitude smaller than the range manifested in the silica gels used in the experiments. The molecular weight of the model polymers is likewise about an order of magnitude smaller than the average value of Mn attributed to the actual polymers. Thus, in using the model calculations to interpret the experimental results, we are assuming that the observed effects depend only on the relative, and not on the absolute, size of the molecules involved.

The effect of the silica gel was examined by comparing simulations where the nonbond interactions (electrostatic and Van der Waals forces) between the silica and the polymer were turned on (polymer/silica blend) to identical simulations where these interactions were turned off (pure polymer). The corresponding mass loss rates, determined by numerical differentiation of the mass of polymer degradation fragments diffusing out of the unit cell as a function of time, are compared in Figure 5. The uncertainties in these rates, estimated from the average standard deviation of the differences in the rate of mass loss obtained from independent simulations performed at the same temperature, are 0.07 and 0.05 (in units of fractional mass loss per 10^{-12} s) for the pure polymer and the blend, respectively. The interactions between the polymer and silica appear to have a stabilizing effect that would be expected to result in a reduction in flammability. A detailed review of the computer

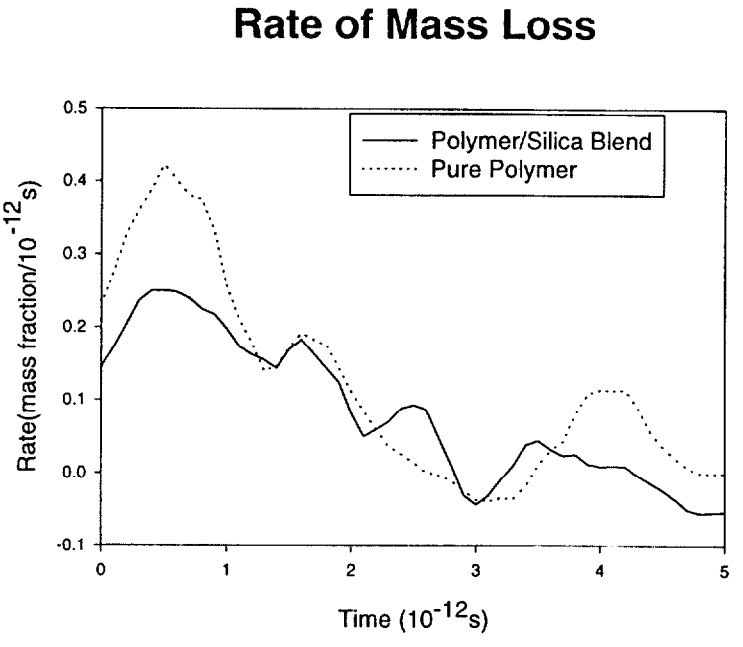

animations of the corresponding trajectories suggests further that the fragments from the degrading polymers tend to get trapped in the pores of the silica. This effect is apparent in

Small Pore Silica

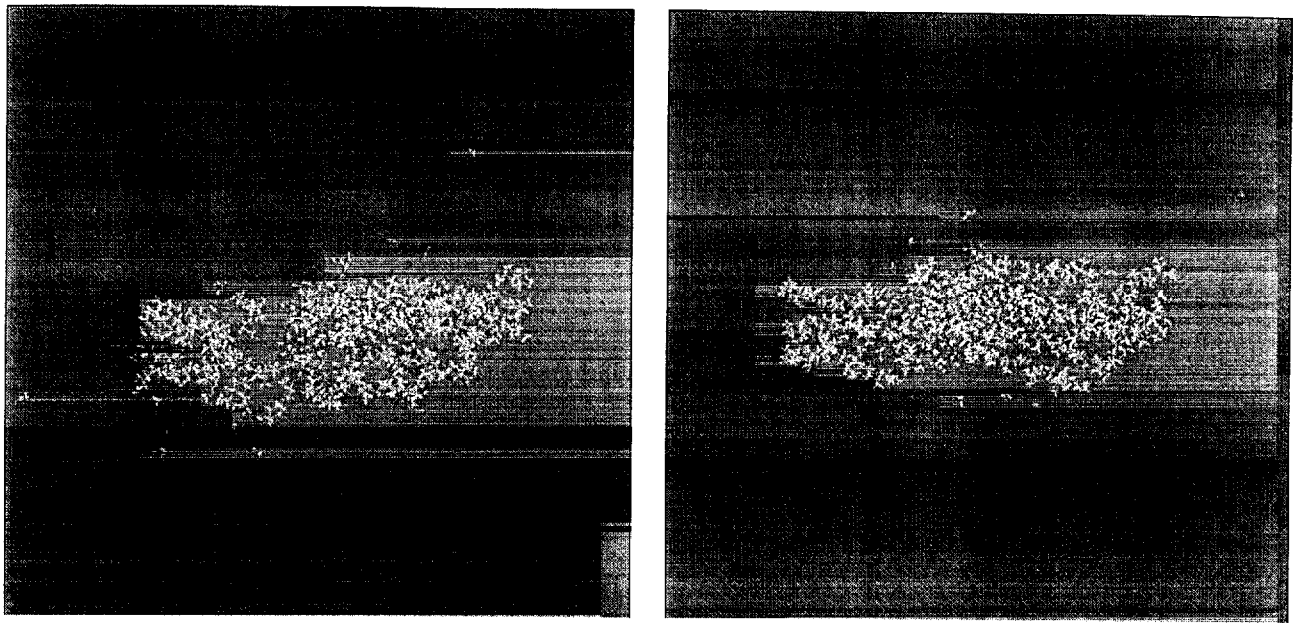

Figure 6. Thermal degradation of pure polypropylene (left) and the blend (right).

Large Pore Silica

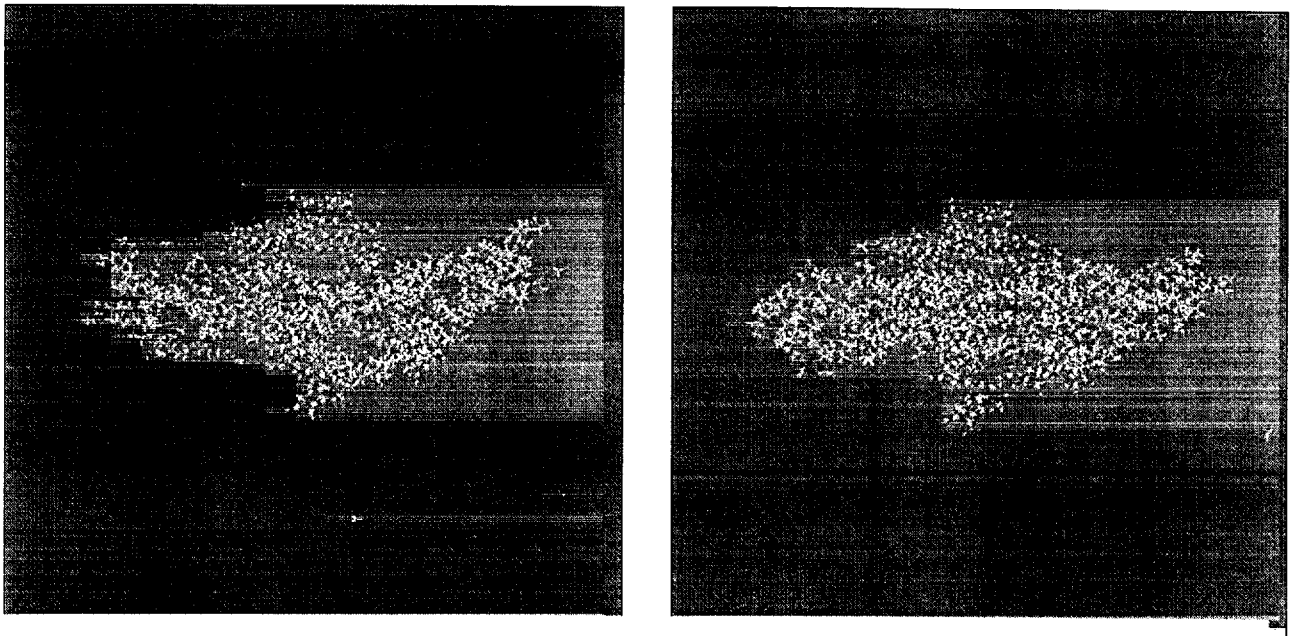

Figure 7. Thermal degradation of pure polypropylene (left) and the blend (right).

Figures 6 and 7 where the last frames from simulations of the thermal degradation of polypropylene in the presence (right) and absence (left) of the silica gel are compared for the small and large pore silica, respectively. In general, the large pore silica appears to be more effective because it can trap a greater mass of polymer degradation products than the small pore silica.

Nanocomposites

Simulated thermal degradation experiments were performed to investigate, at a molecular level, the source of the dramatic increase in fire resistance that has been observed for some polymer nanocomposites [14,15]. The model of the polymer nanocomposite consisted of the 4 polypropylene chains used in the previous study situated above a graphite sheet constructed from about 600 carbon and 80 hydrogen atoms that were used to terminate the edges.

A series of nanocomposite structures with the polymer intercalated between graphite layers separated by a variable distance, b, was obtained by annealing the model polymer and graphite inside of a unit cell with the following dimensions: a = 10.0, c = 3.0 and b = 2.5, 2.8, 3.0, 3.2 and 5.0 nm. The same models of the polymer and graphite were used in all of the structures. That is, only the distance between the graphite sheets and, consequently, the density of the composite was allowed to change from one simulation to the next. The b = 3.0 nanocomposite is displayed in Figure 8.

The simulated annealing was performed as follows. The polymer/graphite assembly was heated at 500 K for 100 time steps of molecular dynamics and then allowed to relax during 100 iterations of the Polak Ribiere conjugate gradient minimization. After 10 cycles, an optimized conformation was obtained by minimizing the full CVFF energy until the maximum derivative was less than 4.2 J/(mol Å). This process was repeated until the energy of the last optimized conformation was the lowest value attained during the course of the simulated annealing procedure.

The molecular dynamic simulations were performed using periodic boundary conditions in two stages. In the first stage, a population of free radical polymer fragments was generated by integrating the equations of motion over a constant temperature path of 873 K for 0.05×10^{-12} s using the full CVFF force field with cross terms coupling adjacent bonds, angles, and torsions. The bond stretching energies and forces were scaled by a factor of 0.2 to ensure that there was a sufficient population of free radical fragments to initiate the propagation and termination reactions (*i.e.* depolymerization, hydrogen transfer, chain stripping, cyclization, crosslinking and radical recombination). The bond scale factor was then set back to unity at the onset of the second stage where the propagation/termination reactions were simulated. This stage of the simulation was carried out using the reactive

forcefield described above at 873 K for 5.0 x 10^{-12} s. The positions and connectivities of the carbon and hydrogen atoms in the graphite were fixed throughout the simulations.

Polypropylene/Graphite Nanocomposite

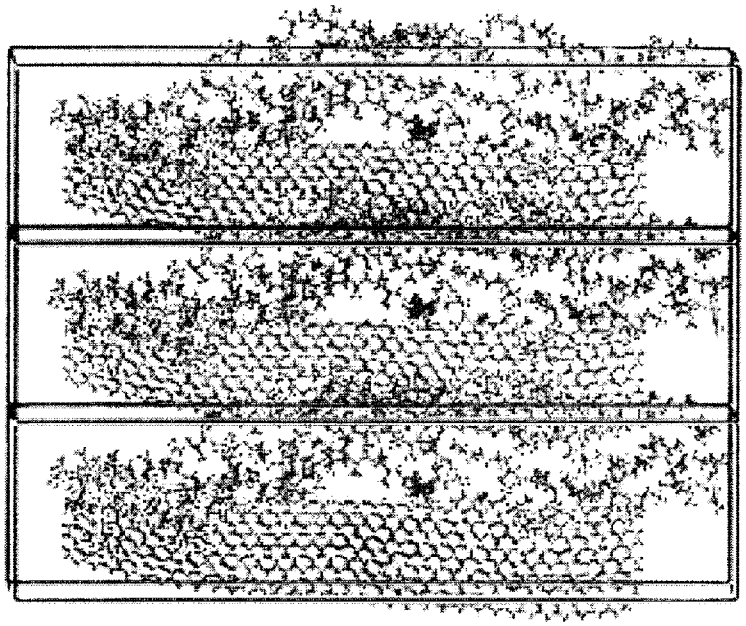

Figure 8. Periodic display of the model polypropylene/graphite nanocomposite.

The relative thermal stabilities of the polypropylene/graphite nanocomposites were assessed by comparing the average rate of mass loss of the model polymer as a function of the distance of separation between the graphite sheets. The effect of the interactions between the polymer and the graphite was analyzed independently from the effect of nano-confinement on the polymer. This was accomplished by comparing the results obtained from simulations where the nonbond interactions between polymer and graphite were turned-on to the corresponding values obtained when these interactions were turned-off.

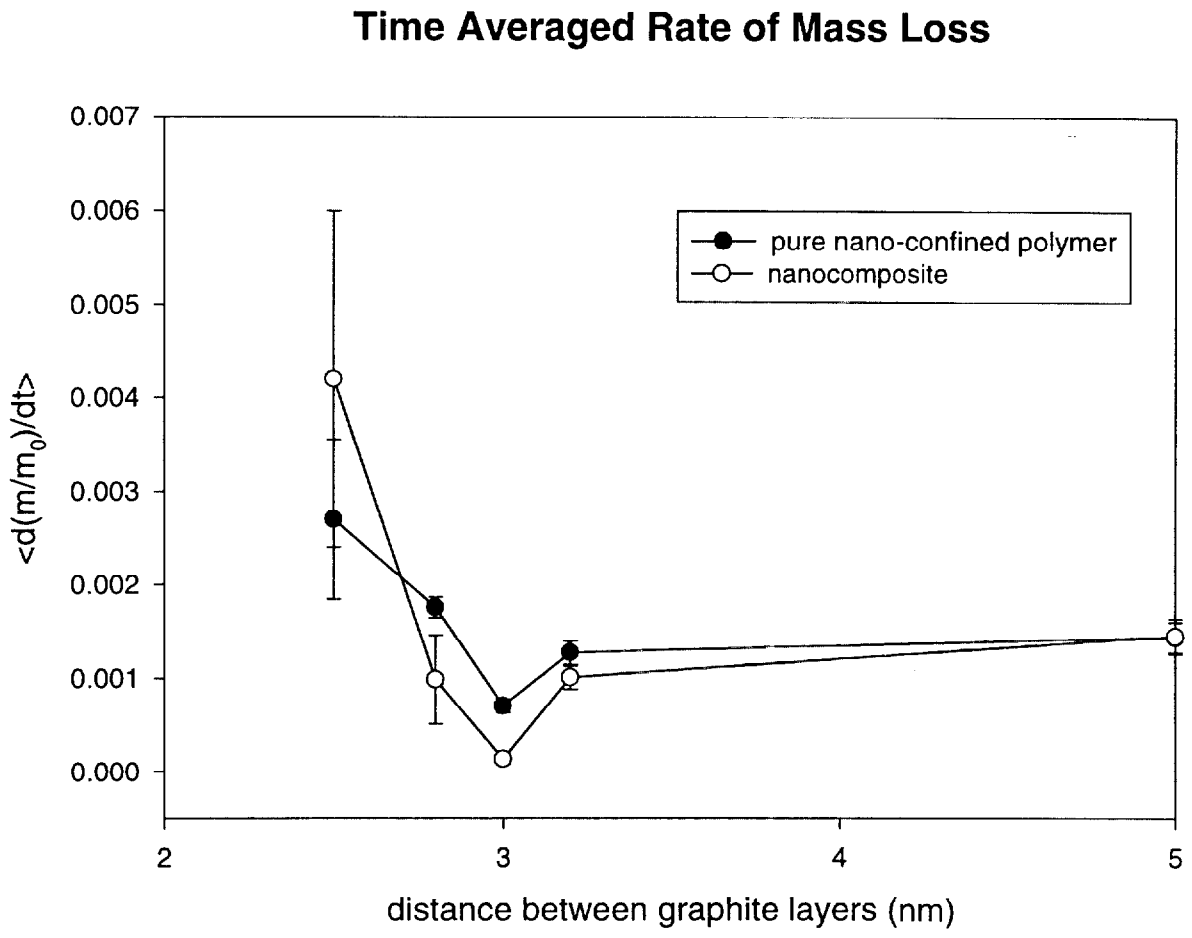

Figure 9. The average rate of mass loss as a function of the distance between the graphite sheets.

The average rate of mass loss for both the pure nano-confined polymers and the nanocomposites are plotted as a function of the distance of separation between the graphite layers in Figure 9. These values were obtained as the arithmetic means of the 51 instantaneous values corresponding to the ensemble averaged rate of mass loss for each of the nanocomposite structures. The uncertainties in these values, depicted as error bars, are the standard deviations of the time averaged rates from 3 simulations corresponding to independent realizations of the initial momentum distribution. The stabilization of the polymer is most pronounced in the b = 3.0 nm nanocomposite and approaches zero at b = 5.0

nm, when the graphite layers are too far apart for there to be a significant interaction between them. At these large distances of separation, the interactions are almost exclusively between the polymer and the graphite. This should approximate what occurs in the delaminated nanocomposites where the graphite layers are individually dispersed in the polymer matrix. The reduction in the average rate of mass loss from the b = 2.8, 3.0 and 3.2 nm nanocomposites, with respect to the pure polymer, is consistent with the results obtained from cone calorimeter experiments on intercalated polypropylene and polystyrene nanocomposites [14].

The observation that the thermal stability of the polymer increases when it is intercalated but is not affected by the presence of the graphite when the layers delaminate is consistent with thermogravimetric data that indicate that intercalated nanocomposites are more thermally stable than delaminated nanocomposites [14,15]. Indeed, Gilman *et. al.* noted that the derivative thermogravimetric (DTG) curves obtained from the delaminated nylon-6/clay nanocomposites are almost identical to the values corresponding to pure nylon-6, whereas the peaks in the DTG of intercalated polystyrene/clay nanocomposites are shifted by 50 ^{0}C from the pure polymer [15]. The fact that the delaminated nylon-6/clay nanocomposites exhibit a reduction in flammability comparable to what is observed for the intercalated nanocomposites, even though the DTG results indicate that polymers are not stabilized when present in delaminated nanocomposites, suggests the possibility that the clay layers reorganize after some of the polymer is gasified. That is, the nanocomposite undergoes a phase change from a delaminated to an intercalated structure as a result of the change in composition brought about by the thermal degradation of the polymer. Once the intercalated nanocomposite is formed, it is stabilized by the mechanism discussed in the preceding paragraphs. This hypothesis is supported by transmission electron microscopy (TEM) of the char that remained after burning samples of the delaminated nylon-6/clay nanocomposites under a thermal flux of 35 kW/m^2 on the cone calorimeter. The TEM images clearly reveal an organized layered structure that was not present prior to combustion [14,15].

Bromine-Containing Fire Retardant Additives

A series of computer simulations were performed on polypropylene in the presence of some representative bromine-containing fire retardants. These included an aromatic compound, decabromobiphenyl, and two aliphatic hydrocarbons, tetrabromoethylene and a vinyl bromide oligomer. The purpose of this study was to make a qualitative comparison of the thermal degradation products and, thereby, to gain further insights into the nature of the mechanisms by which these additives affect a reduction in the flammability of the polymer. The procedures followed in this study were the same as described above in the case of the silica gel additives, except that all of the degrees of freedom, including the atoms that comprised the additives, were dynamic.

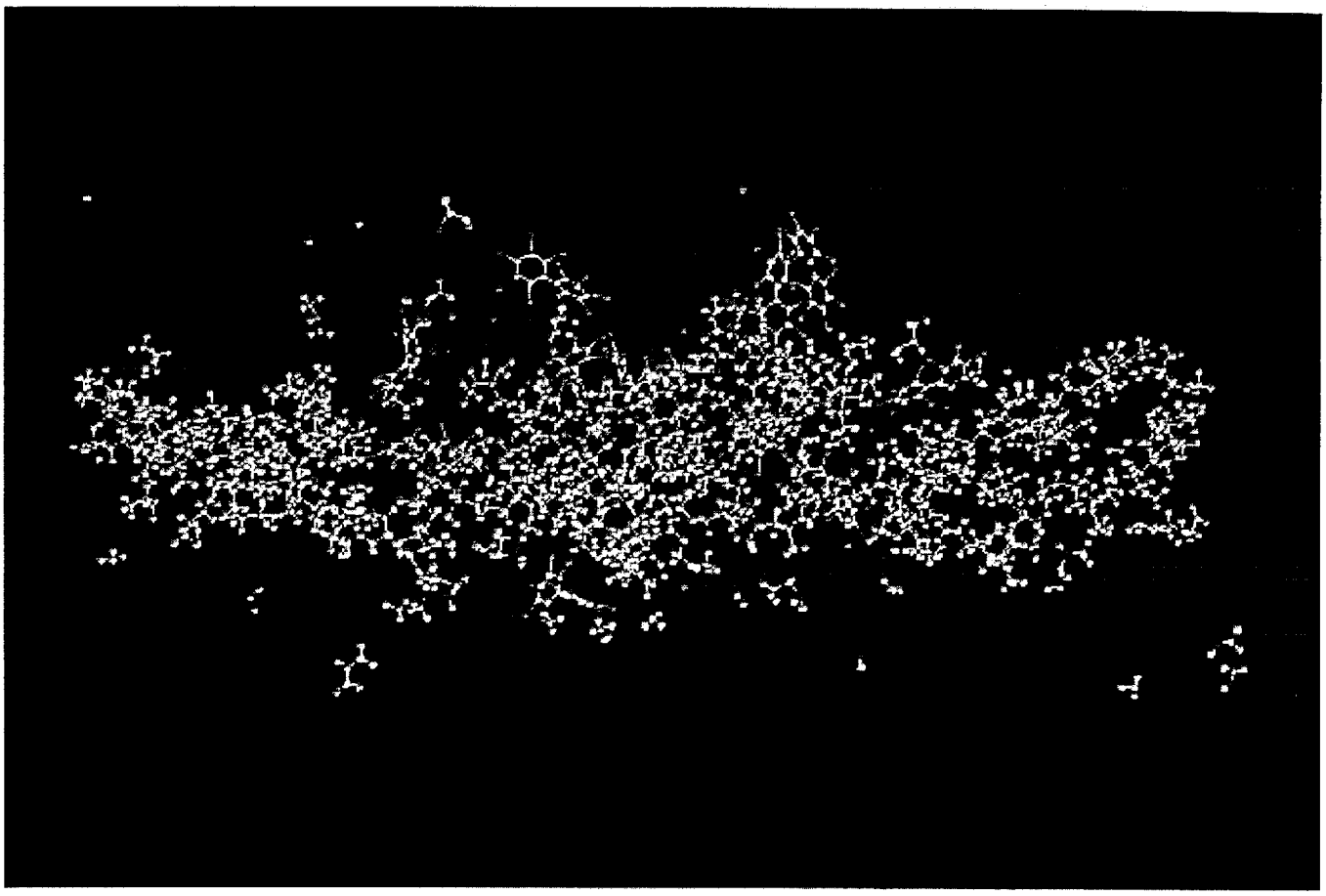

Figure 10. Thermal degradation of a blend of polypropylene with some brominated fire retardants.

Bromine, in the form of Br, Br_2, and small gas phase hydrocarbons, was released early in the simulations. These products are apparent in Figure 10, which is a still frame from the simulated thermal degradation of a polypropylene blend containing both decabrombiphenyl and vinyl bromide oligomer. Additional simulations performed on the additives in the absence of the polymer indicated that Br_2, as opposed to HBr, is a major product of the thermal degradation of both decabromobiphenyl and tetrabromoethylene. This is in sharp contrast to what we observed in the simulated thermal degradation of the vinyl bromide oligomers. In this case, which should be representative of the general class of alkyl bromides, the major products were monomer and HBr. Large amounts of atomic Br were also released, but the formation of molecular Br in the form of Br_2 was not observed. The significance of

this observation is that Br_2, which is thermodynamically less stable than HBr, can play a role in condensed phase suppression by abstracting hydrogen from the polymer. The free radical polymer fragments produced in these hydrogen abstraction reactions can then cross-link to form a high molecular weight, fire resistant char.

Summary and Conclusions

The theory and implementation of a computer model of thermal degradation in polymers was presented. An analysis, based on the theory of unimolecular reactions, indicates that it should be possible to make quantitative predictions of mass loss rates in the thermal degradation of polymers from a small number of relatively short simulations. A direct test of this hypothesis, and of the predictive capability of the model, was made by comparing the computed rate constant for beta-scission in a small gas phase molecule (n-pentane) to the experimental value at 1250 K. The agreement is encouraging, however, more work is needed to make a definitive comparison.

Additional simulations were performed to study the effects of fire retardant additives on the thermal degradation of polypropylene. Included in this survey were blends of polypropylene with silica gel, three representative bromine-containing additives, and a polypropylene/graphite layered nanocomposite. The results, although qualitative in nature, are consistent with experimental findings and, at the same time, provide new insights into the mechanisms by which these additives affect a reduction in the flammability of the polymer.

Acknowledgements

The author is grateful to Dr. Wing Tsang (NIST) for suggesting the kinetic study of pentyl radical. MD_REACT was developed as part of a Cooperative Research and Development Agreement between NIST and MSI (CRADA: CN-1241). Partial support for this work was provided by the Federal Aviation Administration under Interagency Agreement DTFA003-92-Z-0018 monitored by Dr. Richard E. Lyon and from the Industrial Consortium for Environmentally Friendly Flame Retardants.

References

1. M.R. Nyden and D.W. Noid, Phys. Chem. **95**, 940 (1991).

2. M.R. Nyden, G.P. Forney and J.E. Brown, Macromolecules 25, 1658 (1992).

3. M.R. Nyden, J.E. Brown and S.M. Lomakin, Mat. Res. Soc. Symp. Proc. 278, 47

(1992).

4. M.R. Nyden, T.R. Coley and S. Mumby, Polym. Eng. Sci. 37, No. 9 (1997).

5. M.R. Nyden and J.W. Gilman, Computational and Theoretical Polymer Science, in press.

6. Discover 95, Biosym Solutions, 6 (1995).

7. P. Dauber-Osguthorpe, V.A. Roberts, D.J. Osguthorpe, J. Wolff, M. Genest, A.T. Hagler, Proteins: Structure, Function and Genetics 4, 31 (1988).

8. L.S. Kassel, The Kinetics of Homogeneous Gas Reactions, The Chemical Catalog Company, New York, N.Y. (1932).

9. W. Forst, Theory of Unimolecular Reactions, Academic Press, New York, NY (1973).

10. C.F. Cullis and M.M Hirschler, The Combustion of Organic Polymers, Clarendon Press, Oxford, England (1981).

11. Discover User Guide, Part 3, Biosym/MSI, (1995), San Diego.

12. W. Tsang, J.A. Walker, and J.A. Manion, 27th Symposium on Combustion (Int'l), **in press**, (1998).

13. J.W. Gilman, T. Kashiwagi, S. Lomakin, J.D. Lichtenhan, A. Bolf and P. Jones, Additives and Modifiers for Polymers, in press (1998).

14. J.W. Gilman, T. Kashiwagi, S. Lomakin, J.D. Lichtenhan, P. Jones, E. Giannelis and E. Manias, Proceedings of The 6th European Meeting on Fire Retardancy of Polymeric Materials, Lille, France, Sept. (1997).

15. J.W. Gilman, T. Kashiwagi and J.D. Lichtenhan, SAMPE Journal, 33, 40 (1997).

---

* This is a contribution from the National Institute of Standards and Technology and is not subject to copyright.

† Certain commercial equipment, instruments, materials or companies are identified in this paper in order to adequately specify the experimental procedure. This in no way implies endorsement or recommendation by NIST.